



Data-driven virtual sensor for online loads estimation of drivetrain of wind turbines

Omar Kamel^{1,2} · Matthias Kretschmer² · Stefan Pfeifer² · Birger Luhmann² · Stefan Hauptmann² · Carlo L. Bottasso¹

Received: 1 November 2022 / Accepted: 11 January 2023 / Published online: 20 March 2023
© The Author(s) 2023

Abstract

Data-driven approaches have gained interest recently in the field of wind energy. Data-driven online estimators have been investigated and demonstrated in several applications such as online loads estimation, wake center position estimations, online damage estimation. The present work demonstrates the application of machine learning algorithms to formulate an estimator of the internal loads acting on the bearings of the drivetrain of onshore wind turbines. The loads estimator is implemented as a linear state-space model that is augmented with a non-linear feed-forward neural network. The estimator infers the loads time series as a function of the standard measurements from the SCADA and condition monitoring systems (CMS). A formal analysis of the available data is carried out to define the structure of the virtual sensor regarding the order of the models, number of states, architecture of neural networks. Correlation coefficient of 98% in the time domain and matching of the frequency signature are achieved. Several applications are mentioned and discussed in this work such as online estimation of the forces for monitoring and model predictive control applications.

Datengetriebener virtueller Sensor für die Online Abschätzung der Lasten im Antriebsstrang von Windkraftanlagen

Zusammenfassung

Datengetriebene Verfahren haben in letzter Zeit im Bereich der Windenergie an Interesse zugenommen. Dabei wurden datengetriebene Online-Schätzverfahren untersucht und in verschiedenen Anwendungen demonstriert, wie z. B. Online-Lastschätzungen, Schätzungen der Position des Nachlaufzentrums und Online-Schadensschätzungen. Die vorliegende Arbeit demonstriert die Anwendung von Algorithmen des maschinellen Lernens zur Formulierung eines Schätzers für die internen Lasten, die auf die Lager des Antriebsstrangs von Onshore-Windkraftanlagen wirken. Der Lastschätzer ist als lineares Zustandsraummodell implementiert, das durch ein nichtlineares neuronales Netz mit Vorwärtskopplung ergänzt wird. Der Schätzer leitet die Zeitreihen der Lasten als Funktion der Standardmessungen aus den SCADA- und Zustandsüberwachungssystemen (CMS) ab. Es wird eine formale Analyse der verfügbaren Daten durchgeführt, um die Struktur des virtuellen Sensors in Bezug auf die Ordnung der Modelle, die Anzahl der Zustände und die Architektur der neuronalen Netze zu definieren. Es wird ein Korrelationskoeffizient von 98% im Zeitbereich und eine Übereinstimmung mit der Frequenzsignatur erreicht. Zudem werden mehrere Anwendungen erwähnt und diskutiert, wie z. B. die Online-Schätzung von Kräften für Überwachungs- und modellprädiktive Steuerungsanwendungen.

1 Introduction

Data-based modeling approaches play currently a significant role to improve the performance of assets in terms of lifetime extension, reduction of maintenance costs, reduction of downtime, failure prediction of critical and vulnerable components. These objectives can be realized by exploiting the available measurements from the established

✉ Omar Kamel
omar.kamel@mesh-engineering.de

¹ Chair of Wind Energy, Technical University of Munich, Munich, Germany

² MesH Engineering GmbH, Stuttgart, Germany

measurement and control systems on the assets [8]. These measurements are employed to produce an added value to the operation of the asset using machine learning and data analytics techniques. The states and loads estimators, known as virtual sensors, can be incorporated into condition monitoring systems for adequate planning of maintenance to calculate remaining lifetime of mechanical components hence extending the product lifetime. They have been also incorporated into adaptive and modern control algorithms to run the asset efficiently taking into consideration minimization of fatigue damage, minimization of actuators' lifetime consumption.

Recently, considerable work has been directed to tackle the research questions regarding the applications of system identification and machine learning techniques to construct universal estimators that rely mainly on data to be deployed as virtual sensors. [2] developed a virtual sensor of transmitted loads in wind turbine gearboxes using neural networks. The authors achieved coefficient of determination, R^2 , of more than 90% using the proposed methodology. [18] also proposed an online fatigue monitoring estimator using Kalman filters and least square approach and a quasi-static approach based on the low-fidelity simulation model on the intermediate shaft and high-speed shaft of gearbox of wind turbines, where they achieved high coefficient of correlation in the range of 50% to 96%. [16] formulated damage equivalent loads (DEL) estimator on the torque arm of the gearbox housing of wind turbines based on low-frequency SCADA measurements. Several regression algorithms were investigated, yielding correlation-coefficient more than 80%. [5, 6] developed digital twins as state-estimators using Kalman filters to estimate loads on towers using standard SCADA and kinematic measurements, achieving errors of estimations that is less than 8%. On the other hand, [1] highlighted one of the potential applications of using reduced order models and virtual sensors to develop sophisticated control strategies, where they incorporated a reduced order model of the wind turbine into a model predictive controller that attempts to minimize the accumulated damage on the tower root while maintaining compromise between generated power and accumulated damage in the form of economic cost function.

2 Problem Statement

The problem at hand deals with the online estimation of the structural loads endured by the bearings in the drivetrain of onshore wind turbines. This study considers the structural loads on the bearing on front pinion shaft of the drivetrain as an exemplary quantity of investigation.

The development of virtual sensors that can estimate the loads requires several characteristics of the estimator that

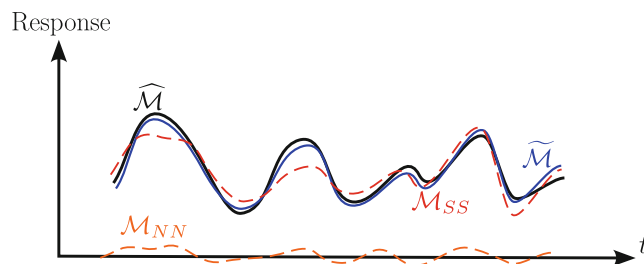


Fig. 1 Qualitative response of the virtual sensor according to Eq. 1

are developed in this work. The virtual sensor should fulfill the following characteristics:

- computational speed and efficiency due to the need of real time estimations,
- minimal, i.e. delivers only the required information,
- can infer the internal states of the system that are neither possible nor easy to measure (e.g. forces and torques),
- is a mathematical dynamical system that can be simulated forward in time and can be used for what-if scenarios and control applications,
- mathematically differentiable that can be used in gradient-based optimization algorithms (e.g. model predictive control frameworks).

3 Methodology

The realization of the attributes mentioned in Sect. 2 of a virtual sensor imposes the implementation of a data-based reduced order model (ROM). The formulation of the proposed concept is based on a reduced-order state-space formulation, which is a linear approximation of the system at hand, which is augmented with a neural network that estimates the error mismatch of the underlying state-space system.

The wind turbine system is inherently non-linear due to for instance the presence of contact between gears or the controller which attempts to maximize the generated power by varying its control variables (the pitch angle and generator torque) that follow a non-linear control strategy based on gain scheduling [15, 22]. Accordingly, having a linear time-invariant reduced representation of the system is not a rational approach. Hence, the need of a more sophisticated system representation is crucial. Thus, the formulation of the virtual sensor presented in this work is based on the assumption that the physical behavior of the investigated dynamical system can be reproduced using an additive es-

imator of reduced state-space (SS) system and a neural network (data-based) model. The combined model reads as

$$\begin{aligned} \widetilde{\mathcal{M}} &\approx \widehat{\mathcal{M}}, \\ \widetilde{\mathcal{M}} &= \mathcal{M}_{SS} + \mathcal{M}_{NN}, \end{aligned} \tag{1}$$

where $\widehat{\mathcal{M}}$ is the system response of the high-fidelity physical model (ground truth), $\widetilde{\mathcal{M}}$ is the estimated system response using the virtual sensor, \mathcal{M}_{SS} and \mathcal{M}_{NN} are the system responses of the linear state-space and neural network models respectively. \mathcal{M}_{SS} can only reproduce the prevalent quasi-static response (so called slow dynamics) of the investigated system due to the reductive nature of the implemented formulation, while \mathcal{M}_{NN} is implemented to be able to estimate the error mismatch between the linear state-space system and the ground truth, which is the transient dynamics arising from higher-order dynamic nonlinearities such as excitation due to gear contact. The qualitative overall system response is depicted in Fig. 1.

3.1 State-space Formulation

The state-space modeling approach is based on the canonical linear time-invariant dynamic system representation with m inputs, q outputs and n state variables, which reads

$$\begin{aligned} \dot{\mathbf{x}} &= \mathbf{A}\mathbf{x} + \mathbf{B}\mathbf{u} \\ \mathbf{y} &= \mathbf{C}\mathbf{x} + \mathbf{D}\mathbf{u}, \end{aligned} \tag{2}$$

where $\mathbf{x} \in \mathbb{R}^n$ is the states vector, $\mathbf{y} \in \mathbb{R}^q$ is the output vector, $\mathbf{u} \in \mathbb{R}^m$ is the input vector. $\mathbf{A}^{n \times n}$, $\mathbf{B}^{n \times m}$, $\mathbf{C}^{q \times n}$, $\mathbf{D}^{q \times m}$ are the state, input, output, feedthrough matrices respectively. For dynamic systems, \mathbf{D} is set to $\mathbf{O}^{q \times m}$ by default, meaning that the system has no feedthrough.

The choice of the model order (size of $\mathbf{x} \in \mathbb{R}^n$ in Eq. 2) is done according to the Hankel singular-values of the available time data. These singular-values define the “energy” of each state in the system. The Hankel singular-values are defined as [4]

$$\sigma_H = \sqrt{\lambda_i(PQ)}, \tag{3}$$

where P, Q are the controllability and observability Gramians of the system, and σ_H is the Hankel singular-value associated with the eigenvalue λ_i . The highest six Hankel singular-values captured more than 90% of the energy of the high-fidelity system, leading to compromise between quality of estimations and complexity of the identified model, which lead to selecting the order of the model to be in the range $n = 4-6$.

3.2 Neural Network Model

Feed-forward neural networks are implemented to construct the second element of the virtual sensor. Neural networks, according to the universal approximation theorem, can represent a wide variety of the underlying functions when given appropriate weights and internal parameters [7, 12, 17].

The neural network is used to predict only the error mismatch between the ground truth and the linear state-space system, i.e.

$$\begin{aligned} e_{SS} &= \widehat{\mathbf{y}} - \widetilde{\mathbf{y}}_{SS} \\ \widetilde{e}_{SS} &= f(\mathbf{u}, \widetilde{\mathbf{y}}_{SS}), \end{aligned} \tag{4}$$

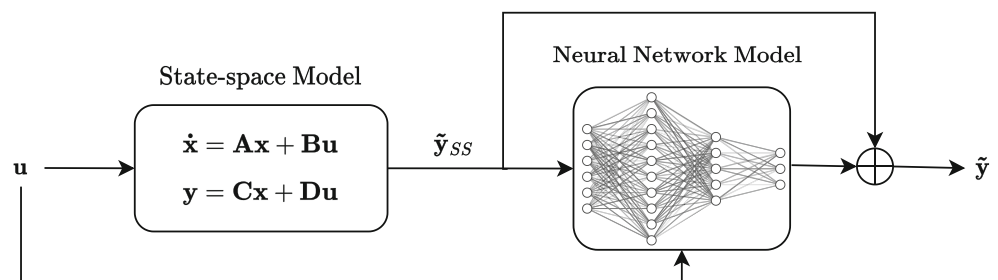
where $\widehat{\mathbf{y}}$ is the ground truth, $\widetilde{\mathbf{y}}_{SS}$ is the output estimation of the state-space system, and accordingly e_{SS} is the error of between the ground truth and the state-space system estimation, \widetilde{e}_{SS} is the estimated error using the neural network, and f is the trained neural network.

The feed-forward neural networks are inherently not able to reproduce dynamic systems behavior due to the absence of state derivatives and/or history of inputs or outputs. However, this can be handled by explicitly feeding in time history as exogenous inputs, in the form:

$$y^k = f(\mathbf{u}^k, \mathbf{u}^{k-1}, \dots, \mathbf{u}^{k-n}), \tag{5}$$

where y^k is the output at timestep k , $\mathbf{u}^k, \mathbf{u}^{k-1}, \dots, \mathbf{u}^{k-n}$ are the inputs at timesteps $k, k-1, \dots, k-n$ in which n previous timesteps are considered. This approach is very simple compared to other approaches that inherently handle the time dependence of dynamic systems such as recurrent neural networks (RNN), gated recurrent units (GRU) and long-

Fig. 2 Gray-box model in deployment with an example deep neural network



short term memory networks (LSTM), which are very complex and problematic during training and deployment [11].

After investigating the effect of shifting the inputs in time and feeding them to the network exogenously, a shallow (one layer) feed-forward neural network of lag = 2 (\mathbf{u}^{k-1} , \mathbf{u}^{k-2} in Eq. 5) with 10 neurons with sigmoid activation function was trained and deployed afterwards.

3.3 Gray-box Model

Following the identification of two building blocks, namely the state-space and neural network models separately, both models are combined in the gray-box model to construct the virtual sensor as demonstrated in Fig. 2 and Eq. 6.

$$\tilde{\mathbf{y}}^k = \tilde{\mathbf{y}}_{SS}^k(\mathbf{u}^k) + \tilde{\mathbf{e}}_{SS}(\tilde{\mathbf{y}}_{SS}^k, \mathbf{u}^k, \mathbf{u}^{k-1}, \mathbf{u}^{k-2}). \quad (6)$$

The proposed approach is applied to estimate the axial force on the frontal bearing of the pinion shaft in the drivetrain, $F_{PS,F,x}$.

4 Implementation

4.1 Modeling and Simulation

The simulations in this study are executed using the IEA Task 37 3.4 MW onshore wind turbine [3]. The wind turbine configuration is summarized in Table 1. A multibody system (MBS) simulation model is set up using the commercial MBS package *Simpack* [9] where different load cases are investigated using simulated turbulent wind conditions in accordance with the IEC 61400-1 [13] standard. *Simpack* has been validated in comparison to other state-of-the-art modeling software such as FAST, HAWC2 (e.g. [20, 21]).

The MBS model is used to generate a time-series of the inputs and outputs of the model that are used afterwards in training and fitting of the corresponding data models as depicted in Fig. 3 which summarizes the work flow of

Table 1 Summary of the configuration of 3.4MW wind turbine [3]

Parameter	Value	Unit
Wind class	IEC 3A	[-]
Rated aerodynamic power	3	MW
Hub height	110	m
Cut-in wind speed	3	ms ⁻¹
Cut-out wind speed	25	ms ⁻¹
Rotor diameter	130	m
Rated rotor speed	11.753	rpm
Rated wind speed	9.8	ms ⁻¹
Gear ratio	97	[-]

data generation. Fig. 4 demonstrates the 3D model of the wind turbine and the detailed model of the drivetrain with the component under consideration and the corresponding coordinate system.

The high-fidelity MBS model features flexible modeling of tower, blades, low speed shaft, high speed shaft using linear beam finite elements. Flexible contact between gears is considered analytically using the Steiner method [10]. Inflow aerodynamics is considered using blade element momentum theory through the coupling of the *AeroDyn* solver [19]. Rotational bearings are modeled using linear stiffness and damping elements. Cross coupling of stiffness forces is considered in the main bearings. The MBS model provides data with sampling frequency of 1000Hz.

4.2 Data Processing and Analysis

Conditions of power production design load cases (DLC 1.2 & 1.3) according to [13] are considered for the data generation. Wind profiles with normal turbulence (NTM) for DLC 1.2 and extreme turbulence (ETM) for DLC 1.3 were generated using *TurbSim* [14], with 2 seeds for each DLC for the nominal wind velocities: [3, 6, 9, 12, 15, 18, 21, 23, 25]ms⁻¹. Additional misaligned inflow design conditions of $\pm 8^\circ$ yaw misalignment at rated

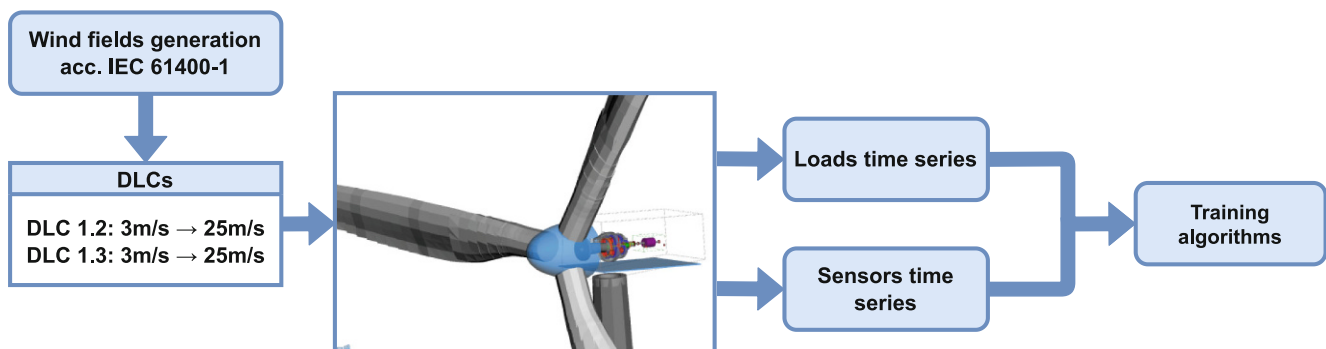


Fig. 3 Workflow of the proposed approach [2]

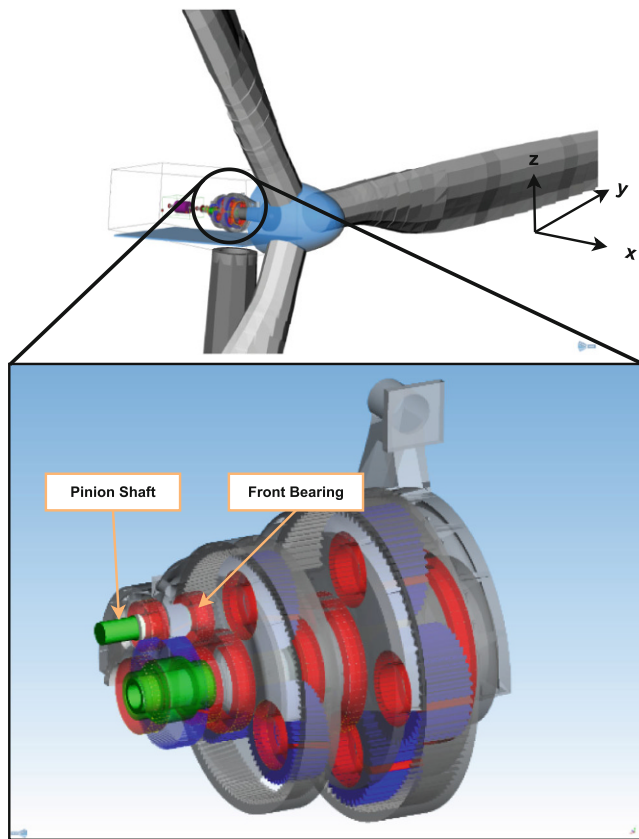


Fig. 4 3D diagram of the wind turbine with the detailed model of the drivetrain from Simpack showing the coordinate system and the component under consideration

wind speed are considered in the analysis, yielding 40 simulations totally, each of 600s long. The load cases are summarized in Table 2.

For training and fitting of the state-space and neural network models the first seed was used, while the second seed was used for testing and validation purposes. Three state-space models were trained using the dataset from DLC 1.3 with wind speeds: [3, 12, 21] m s⁻¹. The trained models were combined into one state-space model using statistically weighted means of the parameters of the individual models. The combination was done using the covariance matrices of the **A**, **B**, **C** matrices of the individual state-space models from each DLC, where these covariance matrices indicate the uncertainty of the individual models. The fitting and training of the neural network was done using

the other DLCs that were not used for fitting the state-space models to avoid data leakage and overfitting.

5 Results and Discussion

The proposed approach is implemented on one output quantity exemplarily, namely the axial reaction component on the front bearing of the pinion shaft, $F_{PS,F,x}$. The inputs to the virtual sensor considered for the investigated output quantity are $\mathbf{u} = [\omega_{Gen} \ P_{elec} \ \mathbf{a}_{PS,F} \ \mathbf{a}_{TT} \ \alpha_{PS,F,x}]$, which are typically the available and accessible physical measurements from the SCADA and CMS systems, where ω_{Gen} is the generator rotational speed, P_{elec} is the generated electric power, $\mathbf{a}_{PS,F}$ are the measured translational acceleration of the front pinion shaft in the directions x, y, z . \mathbf{a}_{TT} is the tower tip translational acceleration in the directions x, y, z , and $\alpha_{PS,F,x}$ is the rotational acceleration of the front bearing of the pinion shaft around the rotational axis x .

The validation of the proposed virtual sensor concept is presented using comparison between the ground truth, which is generated using the high-fidelity simulation tool Simpack, the trained linear state-space model, and the proposed concept of augmenting the simplified linear model with neural networks.

Fig. 5 exhibits the statistical distribution of the normalized with reference to the mean of the reference time series output $\hat{F}_{PS,F,x}$ vs the estimations using state-space model and neural network augmented state-space model. The state-space model (light green) can in most cases reproduce the median of the distribution accurately, however the 25th and 75th percentiles are deviating systematically, while the neural network (light coral) can accurately reproduce the median, the 25th and 75th percentiles and the minimum and maximum ranges of the data with minimal deviations. The deviations observed in the case of $\bar{v}_w = 3 \text{ m s}^{-1}$ can be explained as follows. The cut-in wind speed of the investigated turbine is 3 m s^{-1} , where the controller ramps up the turbine till it reaches the rated rotational speed, hence highly non-linear behavior of the commanded generator torque is present, which leads to larger deviations in the estimations of the virtual sensor compared to the reference signals.

In order to have deeper understanding of the quality of the proposed concept, correlation of the regression is investigated. Pearson’s coefficient of correlation is used as an

Table 2 Summary of load cases

DLC	Wind Speeds [m s ⁻¹]	Turbulence Model	No. of Seeds	Notes	Total No. of Simulations
1.2	3, 6, 9, 12, 15, 18, 21, 23, 25	NTM	2	–	18
1.2	9.8	NTM	2	Yaw misalignment = ±8°	4
1.3	3, 6, 9, 12, 15, 18, 21, 23, 25	ETM	2	–	18

Fig. 5 Statistical box plot of DLC 1.2 for different wind speeds and yaw conditions of the normalized output variable. Color code: Simpack (blue), Linear State-Space (green), Augmented State-Space and Neural Network (Proposed approach) (red)

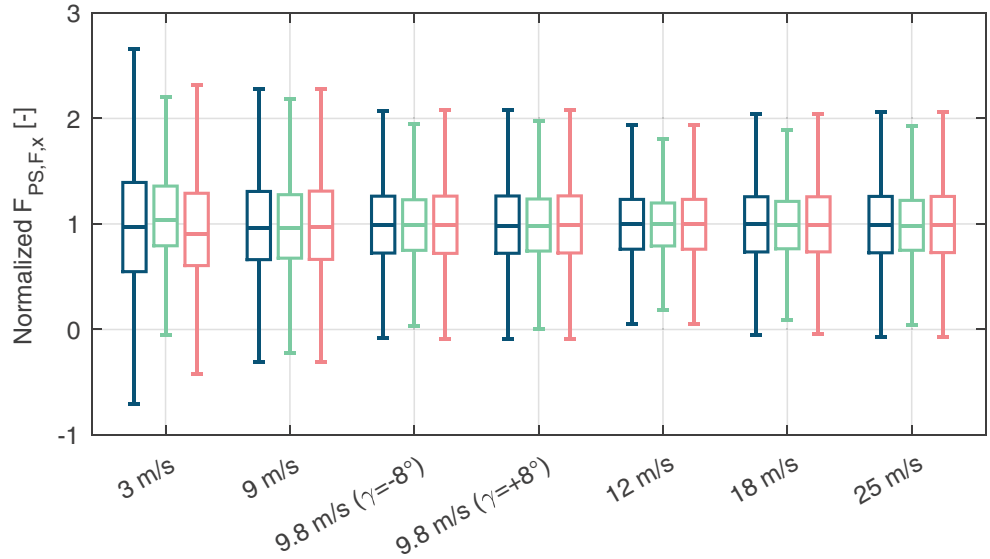


Fig. 6 Correlation between estimations and reference signals for 2 DLCs, x-axis represents the reference signal and y-axis represents the estimations of the virtual sensor. **a** DLC 1.2, $\bar{v}_w = 18\text{m s}^{-1}$, **b** DLC 1.3, $\bar{v}_w = 6\text{m s}^{-1}$

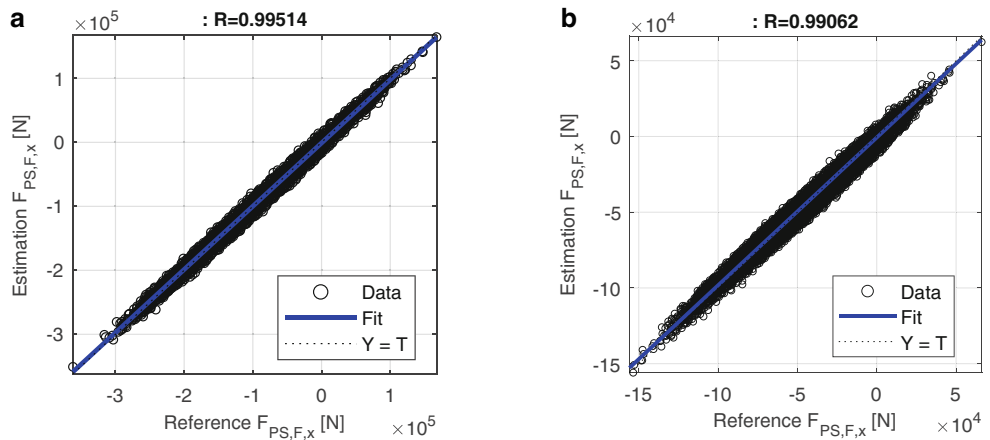
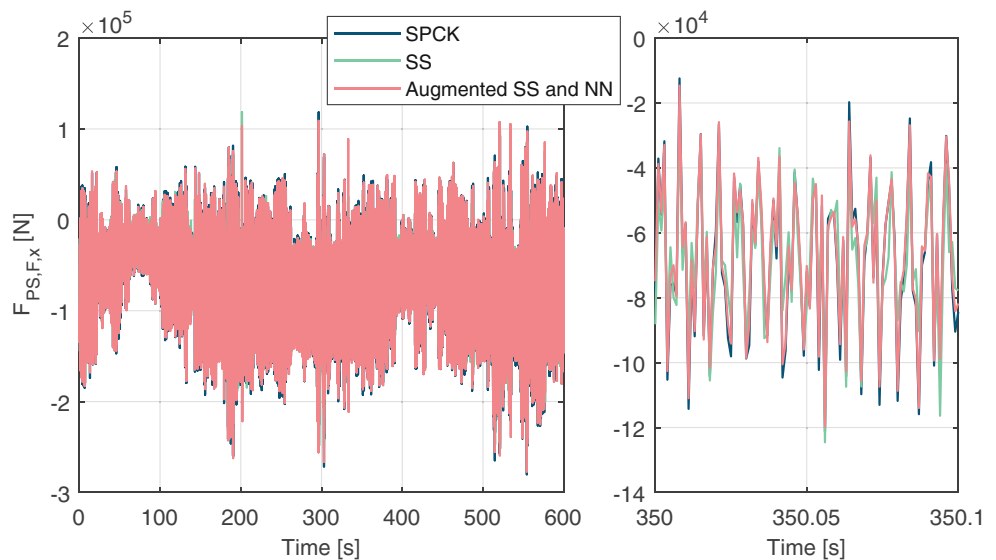


Fig. 7 Estimation vs. ground truth in time domain. DLC 1.2, $\bar{v}_w = 9\text{m s}^{-1}$



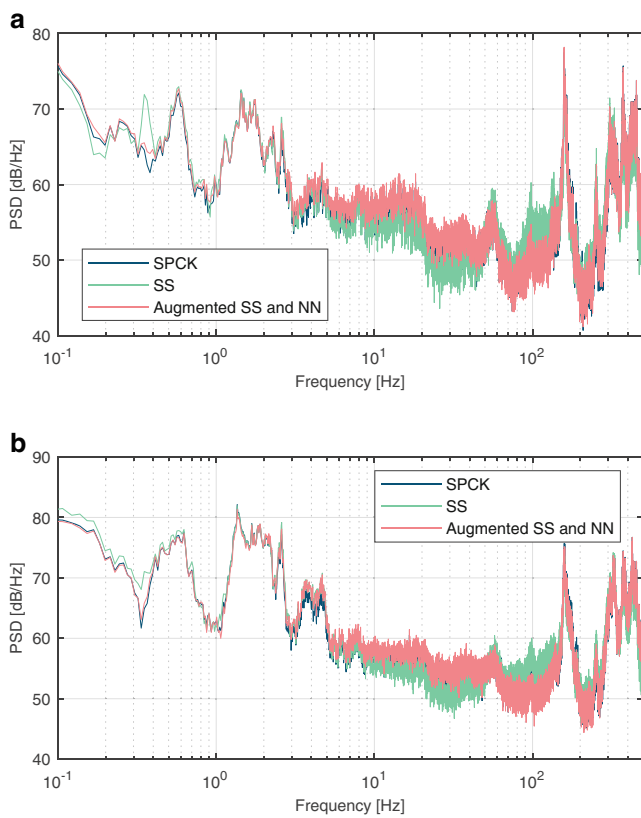


Fig. 8 Power spectral density of estimation vs. ground truth. **a** DLC 1.2, rated wind speed at $\gamma = -8^\circ$, **b** DLC 1.3, $\bar{v}_w = 21 \text{ m s}^{-1}$

error metric, defined as a measure how strong a relationship is between two variables, which reads

$$r_{xy} = \frac{\sum_{i=1}^n (x_i - \mu_x)(y_i - \mu_y)}{\sqrt{\sum_{i=1}^n (x_i - \mu_x)^2} \sqrt{\sum_{i=1}^n (y_i - \mu_y)^2}}, \quad (7)$$

where x_i and y_i are the sample points, n is the number of samples in population, and μ_x, μ_y are the mean of the population.

The regression of two load cases is demonstrated in Fig. 6, achieving 99% coefficient of correlation.

The investigation of the signals in the time and frequency domain helps understand the nature of the quantity to be predicted. Fig. 7 shows the reference signal and the estimated signals of DLC 1.2 for wind speed $\bar{v}_w = 9 \text{ m s}^{-1}$ and an extract of 0.1 s. The linear state-space model does not capture the time-domain behavior well in comparison to the augmented state-space and neural network approach.

Fig. 8 illustrates the power spectral density of two load cases, namely DLC 1.2 at rated wind speed $\bar{v}_w = 9.8 \text{ m s}^{-1}$ with yaw misalignment $\gamma = -8^\circ$ and DLC 1.3 with wind speed $\bar{v}_w = 21 \text{ m s}^{-1}$. The virtual sensor is capable of capturing the complete frequency response of the dynamic system with minimal mismatch.

6 Conclusion and Further Work

In this work a formulation of data-based virtual sensor was achieved which can estimate the internal forces on mechanical components, namely the front bearing of the pinion shaft, with correlation reaching 99% in time and frequency domains. The proposed formulation is based on the augmentation of a linear state-space model with a non-linear feed forward neural network. The data used for fitting and training of the virtual sensor elements were generated using a high-fidelity multibody simulation model of the wind turbine system. Sect. 5 highlights an excerpt of the achieved results.

The virtual sensor can be incorporated into a monitoring framework that can enhance the monitoring capabilities of the standard condition monitoring systems in which it can estimate the internal forces on the mechanical components using the already available and accessible measurements from SCADA and CMS systems. It can also be employed for online vibration monitoring in the frequency domain, where the significant natural frequencies of the system can be identified in an online manner highlighting any abnormal or excessive vibration in the system. In addition to the monitoring purposes, the virtual sensor can be integrated to sophisticated control systems such as model predictive control frameworks, where the virtual sensor can provide measurements of the forces that can be used for optimization purposes such as damage accumulation on the critical mechanical components in order to extend the lifetime of the investigated component or minimize the maintenance costs due to the benefit of prediction of non-measurable quantities.

Funding Open Access funding enabled and organized by Projekt DEAL.

Open Access This article is licensed under a Creative Commons Attribution 4.0 International License, which permits use, sharing, adaptation, distribution and reproduction in any medium or format, as long as you give appropriate credit to the original author(s) and the source, provide a link to the Creative Commons licence, and indicate if changes were made. The images or other third party material in this article are included in the article’s Creative Commons licence, unless indicated otherwise in a credit line to the material. If material is not included in the article’s Creative Commons licence and your intended use is not permitted by statutory regulation or exceeds the permitted use, you will need to obtain permission directly from the copyright holder. To view a copy of this licence, visit <http://creativecommons.org/licenses/by/4.0/>.

References

1. Anand A, Loew S, Bottasso CL (2022) Economic nonlinear model predictive control of fatigue for a hybrid wind-battery generation system. *J Phys Conf Ser* 2265(3):106–32. <https://doi.org/10.1088/1742-6596/2265/3/032106>

2. Azzam B, Schelenz R, Roscher B et al (2021) Development of a wind turbine gearbox virtual load sensor using multibody simulation and artificial neural networks. *Forsch Ingenieurwes* 85(2):241–250. <https://doi.org/10.1007/s10010-021-00460-3>
3. Bortolotti P, Tarres HC, Dykes K et al (2019) IEA wind task 37: systems engineering in wind energy – WP2.1 reference wind turbines <https://doi.org/10.2172/1529216> (<https://www.osti.gov/biblio/1529216>)
4. Boyd S, El Ghaoui L, Feron E, Balakrishnan V (1994) *Linear matrix inequalities in system and control theory*. Society for industrial and applied mathematics
5. Branlard E, Giardina D, Brown CSD (2020) Augmented Kalman filter with a reduced mechanical model to estimate tower loads on a land-based wind turbine: a step towards digital-twin simulations. *Wind Energy Sci* 5(3):1155–1167. <https://doi.org/10.5194/wes-5-1155-2020>
6. Branlard E, Jonkman J, Dana S et al (2020) A digital twin based on OpenFAST linearizations for real-time load and fatigue estimation of land-based turbines. *J Phys Conf Ser* 1618:22030. <https://doi.org/10.1088/1742-6596/1618/2/022030>
7. Brunton SL, Kutz JN (2019) *Data-driven science and engineering machine learning, dynamical systems, and control*
8. Clifton A, Barber S, Bray A et al (2022) Grand challenges in the digitalisation of wind energy. *Wind Energy Science Discussions* 2022, pp 1–42 <https://doi.org/10.5194/wes-2022-29> (<https://wes.copernicus.org/preprints/wes-2022-29/>)
9. Dassault Systèmes (2022) Simpack. <https://www.3ds.com/products-services/simulia/products/simpack/>. Accessed 15.08.2022
10. DIN 3990 (1987) Tragfähigkeitsberechnung von Stirnrädern; Einführung und allgemeine Einflußfaktoren. <https://doi.org/10.31030/2069785>
11. Freire PJ, Srivallapanonndh S, Napoli A et al (2022) Computational complexity evaluation of neural network applications in signal processing <https://doi.org/10.48550/ARXIV.2206.12191> (<https://arxiv.org/abs/2206.12191>)
12. Gedon D, Wahlström N, Schön TB et al (2020) Deep state space models for nonlinear system identification <https://doi.org/10.1016/j.ifacol.2021.08.406>
13. IEC 61400-1 (2005) *Wind turbines – Part 1: Design requirements*
14. Jonkman BJ, Buhl JML (2006) *Turbsim user’s guide* <https://doi.org/10.2172/891594> (<https://www.osti.gov/biblio/891594>)
15. Jonkman J, Butterfield S, Musial W et al (2009) Definition of a 5-mw reference wind turbine for offshore system development <https://doi.org/10.2172/947422> (<https://www.osti.gov/biblio/947422>)
16. Kamel O, Hauptmann S, Bottasso CL (2022) Estimation of damage equivalent loads of Drivetrain of wind turbines using machine learning. *J Phys Conf Ser* 2265(3):32075. <https://doi.org/10.1088/1742-6596/2265/3/032075>
17. Ljung L, Andersson C, Tiels K et al (2020) Deep learning and system identification. *IFAC PapersOnLine* 53(2):1175–1181. <https://doi.org/10.1016/j.ifacol.2020.12.1329>
18. Mehlan FC, Nejad AR, Gao Z (2021) Estimation of wind turbine gearbox loads for Online fatigue monitoring using inverse methods. In: *Ocean renewable energy*, vol 9. American Society of Mechanical Engineers, In <https://doi.org/10.1115/OMAE2021-62181>
19. Moriarty PJ, Hansen AC (2005) *Aerodyny theory manual* <https://doi.org/10.2172/15014831> (<https://www.osti.gov/biblio/15014831>)
20. Popko W, Huhn ML, Robertson A et al (2018) Verification of a numerical model of the offshore wind turbine from the Alpha Ventus wind farm within OC5 phase III 10 <https://doi.org/10.1115/OMAE2018-77589>
21. Popko W, Robertson A, Jonkman J et al (2019) Validation of numerical models of the offshore wind turbine from the Alpha Ventus wind farm against full-scale measurements within OC5 phase III. *J Offshore Mech Arct Eng*. <https://doi.org/10.1115/1.4047378>
22. Wright AD, Fingersh LJ (2008) Advanced control design for wind turbines; part I: control design, implementation, and initial tests <https://doi.org/10.2172/927269> (<http://www.osti.gov/servlets/purl/927269-8Bh5XU/>)